4220 *Macromolecules* **2009**, *42*, 4220–4223
DOI: 10.1021/ma900031u

Macromolecules
ARTICLE

β Phase in Chiral Polyfluorene Forms via a Precursor

Girish Lakhwani and Stefan C. J. Meskers*

Molecular Materials and Nanosystems, Eindhoven University of Technology, P.O. Box 513, NL 5600 MB, The Netherlands

Received January 7, 2009; Revised Manuscript Received April 15, 2009

ABSTRACT: Chiral poly{9,9-bis[(3*S*)-3,7-dimethyloctyl]-2,7-fluorene) shows temperature-induced aggregation in 1-octanol. For polymer concentrations of >0.01 mg/mL and cooling rates of ≤ 10 °C/h, aggregates form, showing characteristics of the β phase of polyfluorene. At higher cooling rates, lower concentration, or both, another type of aggregates forms (α). α and β phases are distinguished by absorption, fluorescence, and circular dichroism (CD) spectroscopy. Temperature-dependent CD and dynamic light scattering show that the β phase forms only via a precursor aggregate, whose formation is concentration-, temperature-, and time-dependent. The yield of the β phase can be optimized by choosing processing conditions that favor the formation of the precursor.

Introduction

Crystallization of macromolecules can be a multistep process. In a number of cases, intermediates present in the early stages of crystallization have been identified such as transient mesophases,[1] precrystalline aggregates,[2] or crystallization precursors.[3] It has been recognized that the final morphology obtained in polymer processing is often imposed by such precursor structures present early on in the crystallization process.[4] For π-conjugated polymers, film morphology directly influences its optoelectronic properties, such as charge carrier mobility and light emission characteristics.[5] Therefore, when trying to optimize these properties, knowledge of precursor structures in the aggregation of π-conjugated chains is of paramount importance. Here we investigate the aggregation of chiral polyfluorene (poly{9,9-bis-[(3*S*)-3,7-dimethyloctyl]-2,7-fluorene, **1**)[6,7] in 1-octanol and distinguish two chiral polymorphs (α and β). For the formation of only one of these polymorphs, we identify a precursor structure. The formation of this precursor is a time- and concentration-dependent process. By choosing processing conditions favorable to precursor formation, one can control which of the polymorphs is formed upon aggregation (α or β).

The polyfluorenes constitute a class of π-conjugated polymers for which organization in solid phase and functional properties have been investigated in considerable detail. For instance, poly (9,9-di-*n*-octyl-2,7-fluorene) (PFO)[8] can form a crystalline phase (α) below 160 °C. Besides this α phase, a mesomorphic β phase has also been identified,[9] which can be induced by, for example, solvent treatment. This β phase can be distinguished from α by its optical properties: the absorption and luminescence band associated with the allowed transition between ground and lowest excited singlet state for β are red-shifted in comparison with those for the α phase. This indicates a larger effective conjugation length for π electrons along the backbone in the β phase, resulting from a special conformation of the polymer backbone.[10] Several processing conditions are known to favor induction of β phase.[9,11] Although a number of characteristic diffraction features have been identified for the β phase in PF derivatives with linear side chains,[12] the structure of the β phase has not yet been resolved, and a detailed mechanistic understanding of its formation is still lacking.

*Corresponding author. E-mail: s.c.j.meskers@tue.nl.

Experimental Section

The polymer used is chiral PF (poly{9,9-bis[(3*S*)-3,7-dimethyloctyl]-2,7-fluorene, **1**) with amino end groups having $M_n \approx 20\,400$ and $M_w \approx 37\,600$ (PDI 1.84). **1** was synthesized by Suzuki polycondensation by close analogy to the procedure reported in literature,[7a] with a small percentage (1%) of *p*-bromonitrobenzene as the end-capper to control the molecular weight. Subsequent reduction by $SnCl_2$ in EtOH/EtOAc led to reduction of the nitro end groups to amino end groups. We prepared stock solutions of **1** by dissolving the polymer in 1-octanol at high temperatures.

CD and LD spectra were measured on a Jasco J-815 spectropolarimeter where the sensitivity, time constant, and scan rate were chosen appropriately. Temperature-dependent measurements were performed with a PFD-425S/15 Peltier-type temperature controller with a temperature range of 263−383 K and a controlled cooling/heating rate. In these temperature-dependent measurements, absorption can be measured simultaneously with the CD. The temperature corresponding to the onset of the CD effect, T_{aggr}, is defined as the temperature at which the CD signal rises above the noise level (≥ 2 mdeg). Unless otherwise stated, CD and absorption spectra pertain to an optical path length of 1 cm. UV−vis absorption measurements at room temperature were done on a Perkin-Elmer Lambda 900 UV/vis/NIR spectrometer. Fluorescence measurements were performed on an Edinburgh Instruments FS920 double-monochromator luminescence spectrometer using a Peltier-cooled, red-sensitive photomultiplier. Scattering experiments were done using a Zetasizer Nano ZS with 632 nm light and detection at an angle of 173° in the temperature range of 283−263 K. We determined equivalent hydrodynamic radii by fitting the Siegert relation[13] including a single exponential decay function to the experimental correlation function. From the decay constant ($\Gamma = Dq^2$), we estimate the hydrodynamic radius using the Stokes−Einstein relation for a spherical particle.

Results and Discussion

To investigate the aggregation of the chiral polyfluorene **1** in 1-octanol, we use temperature- and time-dependent CD. **1** is dissolved in 1-octanol by heating to 90 °C.

At this temperature, the solutions show no significant CD effect (Figure 1), indicating that the polymer chains are present as free random coils. Upon cooling, the solubility of the rigid rodlike

 Published on Web 05/04/2009

polymer is lowered, and chains aggregate. During controlled cooling of the hot solution containing 0.010 mg/mL of polymer at a rate of 10 °C/h, we see the induction of a bisignate CD signal at temperatures $T < 50$ °C. (See Figure 1a.) These CD features are associated with the electronic transition from the ground state to the lowest excited singlet state of the polymer (S_0-S_1). The CD signal reaches a minimum at a wavelength of 350 nm and a maximum at 420 nm. We assign these features to a (semi-) crystalline state of the polymer: α phase.

For polymer with a concentration of 0.014 mg/mL, we find different CD features under the same conditions (Figure 1b). At −10 °C, the CD signal shows minima at 333 and 410 nm and a maximum at 430 nm. This indicates the formation of a different polymorph at high concentration. This polymorph is characterized by a long wavelength shoulder in the absorption spectrum near 425 nm (Figure 2a). This shoulder is also observed for the β phase in achiral polyfluorene. Upon excitation of this phase via this long wavelength transition with 425 nm light, we observe a structured fluorescence spectrum with narrow vibronic bands (Figure 2b). The bands are red-shifted with respect to those from the α phase by about 20 nm. These features are indicative of a highly ordered β phase. Upon heating, the long wavelength shoulder vanishes from the spectrum at $T = 70$ °C (Figure 2c). This marks the melting temperature of the β phase.

Interestingly, we find that the β phase does not form in a single step from the molecularly dissolved state but involves a precursor. This precursor can be observed in the temperature-dependent CD spectra at temperatures near $T = 50$ °C just before the onset of aggregation (Figure 1b). The precursor is characterized by a CD band shape with a single minimum at 410 nm. Importantly, we find that in cooling experiments, the induction of the β phase is invariably accompanied by the occurrence of the precursor in the early stages of aggregation. Under those conditions where the α phase is formed, the precursor is not observed (Figure 1a and the Supporting Information).

The involvement of the precursor in the formation of the β phase can be further illustrated by looking at the CD signal at 416 nm as a function of temperature (Figure 3a). At low concentration (0.006 mg/mL), the CD signal measured at $T = 45$ °C is slightly positive, showing that the precursor does not form under these conditions. Upon further cooling, we observe the formation of the α phase with an onset of aggregation at $T_{aggr} = 40$ °C. Upon further cooling to −10 °C and subsequent heating, this phase melts again at around 50 °C. By contrast, at higher polymer concentration (0.014 mg/mL), the emergence of a negative Cotton effect for $T < 50$ °C indicates the formation of the precursor. Below 40 °C, the negative CD signature for the precursor signature gives way to the positive CD of the β phase. Upon cooling to −10 °C and subsequent heating to 90 °C, we see that the β-phase melts around 70 °C. The large hysteresis indicates that the precursor structures further assemble in a cooperative manner forming the β phase. Consistent with this, the precursor signature is not observed in the heating run of CD experiments. The CD band shape of the β phase hardly changes upon heating to 70 °C,[14] which indicates that this phase is homogeneous on the length scale corresponding to the typical aggregate size. The intensity under the long wavelength shoulder at 425 nm that is the main characteristic of the β phase is only a fraction of the total intensity under the S_0-S_1 absorption band near 390 nm. This low relative intensity, which is also observed for achiral polyfluorene,[15] indicates that not all polymer chains in the β phase may have a backbone conformation with extended conjugation causing the long wavelength absorption. This suggests that the β phase accommodates different backbone conformations and may not be a 'pure' phase at the molecular level.

Time-dependent CD measurements show that the precursor is stable in time at $T = 45$ °C (Figure 3c). At this temperature, the precursor is characterized by a monosignate CD spectrum (Figure 3b). After rapid cooling (>600 °C/h) of the solution containing the precursor from 45 to −10 °C, a CD spectrum results (Figure 3d) that shows some similarity with that of the precursor but is markedly different from that of the β phase

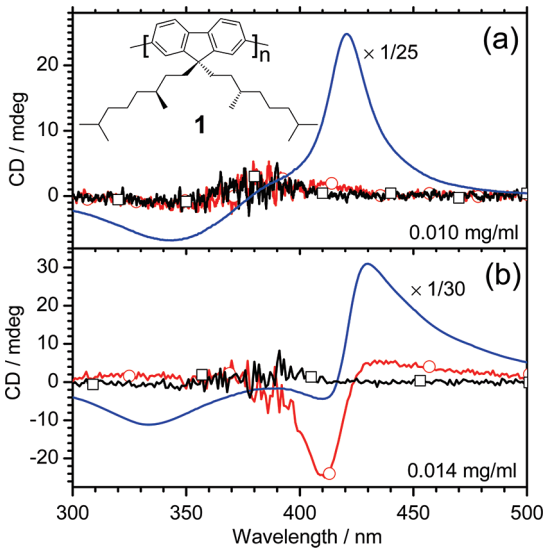

Figure 1. CD spectra of (**1**) chiral PF in 1-octanol at (a) 0.010 and (b) 0.014 mg/mL concentration (bottom) at $T = 90$ °C (−□−), $T = 50$ °C (−○−), and $T = -10$ °C (—) at a cooling rate of 10 °C/h.

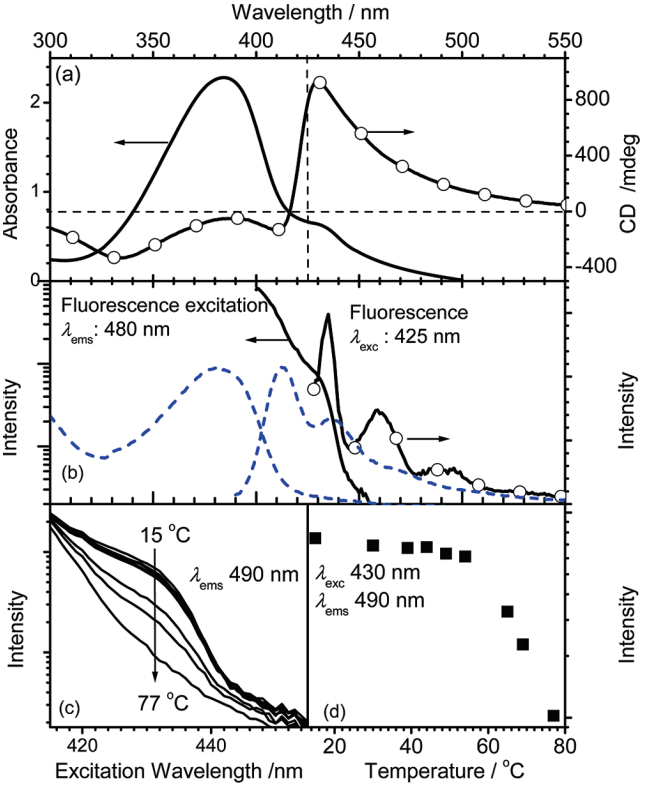

Figure 2. (a) Absorption and CD spectra for **1** (0.014 mg/mL) in 1-octanol at room temperature. (b) Corresponding fluorescence and fluorescence excitation spectra. Wavelength of excitation (425 nm) and of emission detection (480 nm). The blue dashed lines show absorption and fluorescence (excitation at 380 nm) for **1** at 0.001 mg/mL. (c) Temperature dependence of the long wavelength shoulder in the excitation spectrum of **1** as shown in b. Fluorescence monitored at 490 nm. (d) Corresponding fluorescence intensity upon excitation at 430 nm as a function of temperature.

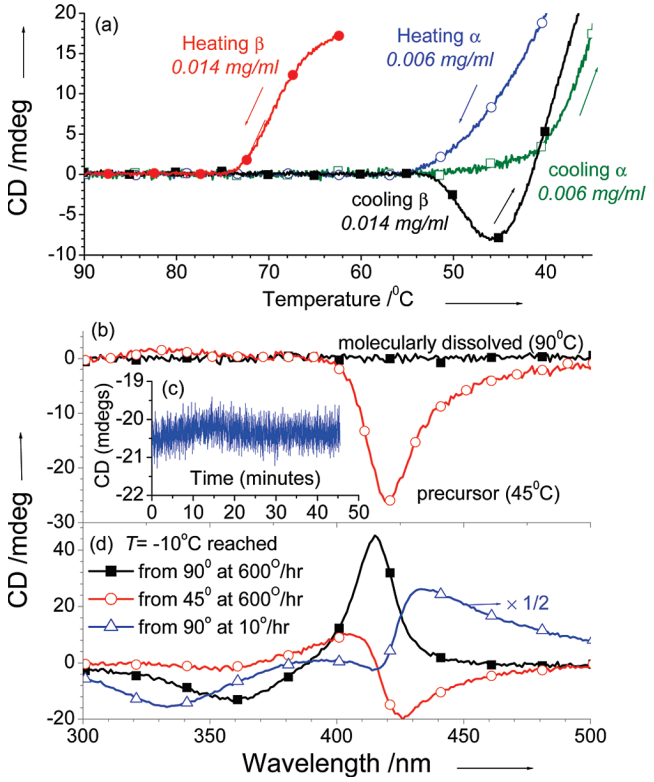

Figure 3. (a) Circular dichroism of **1** in 1-octanol monitored at 416 nm as a function of temperature upon cooling at 10 °C/h from T = 90 to −10 °C. Data for two different concentrations: 0.006 mg/mL (open symbols) and 0.014 mg/mL (filled symbols). (b) CD spectra of **1** at T = 90 and 45 °C (0.04 mg/mL, 1 mm optical path length, cooling from 90 °C at 10 °C/h). (c) Time evolution of the CD at 416 nm and 45 °C. (d) CD spectra at −10 °C upon rapidly cooling (>600 °C/h) the solutions shown in b from 90 °C (−■−) and from 45 °C (−○−). Slow cooling from 90 °C at 10 °C/h (−△−).

(Figure 1b). Therefore, the formation of the β phase from the precursor is a time-dependent phenomenon and may be interpreted in terms of cooperative aggregation of precursor structures. From the same solution, the α phase is obtained when quenching directly from 90 to −10 °C.

Further evidence of the involvement of a precursor in the temperature-induced aggregation of **1** at slow cooling rates comes from dynamic light scattering experiments. Figure 4 illustrates changes in light scattering upon cooling a solution of **1** in octanol (0.33 mg/mL) at fast (60 °C/h) and slow (10 °C/h) cooling rates. As can be seen in Figure 4a at slow cooling rate, the scattered intensity rises above the base level already at a temperature of 64 °C, whereas at fast cooling rates, the onset occurs at lower temperatures. By examining the intensity of scattered light in a broader temperature range (Figure 4b), we observe a distinct shoulder in the temperature range of 64−55 °C upon slow cooling. This is consistent with a biphasic aggregation involving a precursor. At fast cooling, the shoulder is absent. The analysis of the autocorrelation function of the intensity of scattered light for slow cooling (Figure 4c) confirms that in the temperature range of 64−55 °C, small aggregates are formed that grow into larger ones at lower temperature. Taking into account the temperature dependent viscosity and refractive index of 1-octanol,[16] we estimate an average equivalent hydrodynamic radius of the aggregates upon slow cooling of (1 and 2) × 10^2 nm at respectively 57.5 and 20 °C. For fast cooling (Figure 4d), the corresponding numbers are (0.6 and 1) × 10^2 nm. Here the lower value of the correlation function at 1 μs shows that the intensity of light scattered by the aggregates is still comparable to the intensity of light scattered by the solvent.

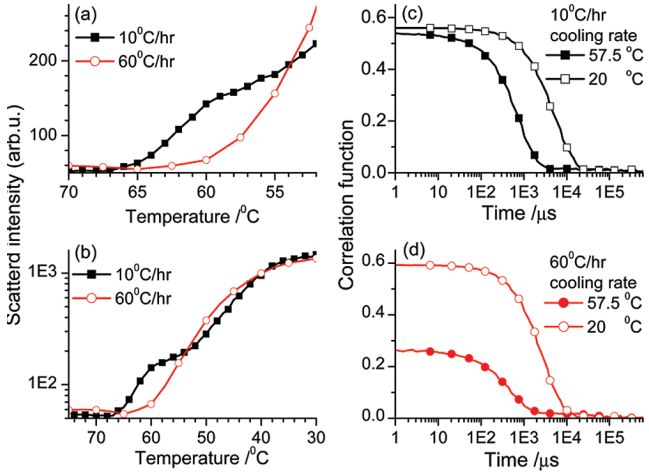

Figure 4. Dynamic light scattering measurements on a solution of **1** in 1-octanol (0.33 mg/mL) upon cooling the solution from 90 °C to room temperature at different cooling rates. (a,b) Intensity of scattered light for cooling rates of 10 °C/h (−■−) and 60 °C/h (−○−). (c,d) Autocorrelation function for the fluctuating intensity of scattered light recorded at 57.5 and 20 °C for cooling rates of 10 °C/h (−■−, −□−, c) and 60 °C/h (−●−, −○−, d).

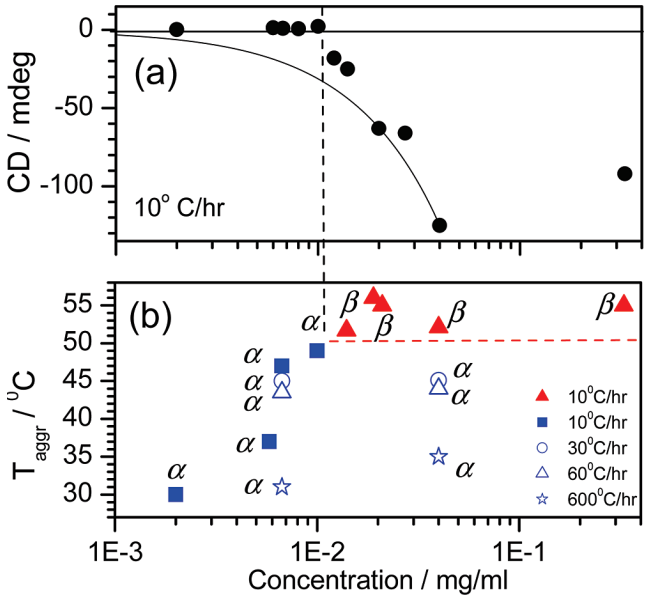

Figure 5. (a) Maximum precursor CD observed at 50 °C in the neighborhood of 416 nm for different concentrations upon cooling from T = 90 °C at a rate of at 10 °C/h. The curved solid line illustrates a linear relation between CD and concentration. (b) Temperature at which the CD signal at 416 nm sets in and the nature of the CD band shape (α/β, see text) upon further cooling to −10 °C at 10 °C/h (filled symbols). Open symbols: corresponding data for faster cooling rates.

The magnitude of the CD effect after cooling to 50 °C as a function of concentration is shown in Figure 5. For concentrations below 0.01 mg/mL, the CD effect is negligible. For concentrations exceeding 0.01 mg/mL, we observe negative CD, marking the formation of precursor. This nonlinear dependence of the negative CD effect from the precursor on concentration shows that precursor formation involves intermolecular interactions between several polymer chains coming together to form the precursor. This is reminiscent of the formation of the triple helix from collagen-mimicking peptides.[17] The monosignate CD band shape of the precursor may be explained by a helical conformation of the backbone of the polyfluorene.[18,19] Diffraction studies[20] and molecular modeling[6,21] on achiral

polyfluorene have indicated that helical conformations approximately described by 5_1 (or 5_2) are particularly stable. For the β phase, helices close to 2_1 have been proposed.[10] The absence of the bisignate CD band shape expected for exciton coupling between chains held in a chiral arrangement[22] can only be explained assuming that in the precursor, the polyfluorene chains are oriented in the same direction. A possible structural model for the precursor could be intertwined helices. Molecular modeling studies on chiral oligofluorene indicate the possibility of such intertwined helices.[23]

At cooling rates exceeding 10 °C/h, the precursor (and β phase) are not formed.[14] This indicates that the formation of precursor is an intrinsically slow process, involving e.g. concerted folding of long random coils. The dependence of β-phase formation is further illustrated in Figure 5b. Here the temperature at which the CD sets is plotted as a function of concentration upon cooling. The character of the aggregates obtained at −10 °C (α/β) is illustrated by the different symbols. As can be seen, the β phase is obtained for concentrations >0.01 mg/mL. This demarcation between α/β formation coincides with the onset concentration for the formation of precursor. The formation of the β phase can also be inhibited by increasing the rate of cooling. For cooling rates of 30 °C/h and higher, the α phase is obtained instead of β.

Conclusions

In summary, we have shown that a particular polymorph (β) of chiral polyfluorene exists whose formation involves a metastable precursor. Because of the fact that the formation of the other polymorph (α) apparently does not proceed via this precursor, one can promote β-phase formation by choosing those processing conditions that favor precursor formation.

Acknowledgment. This research has been supported by The Netherlands Organization for Scientific Research (NWO) through a grant in the VIDI scheme. We thank Dr. R.J. Abbel for the generous gift of polyfluorene polymer. We acknowledge Dr. W.J.E.M. Habraken and Dr. J. Laven for assistance in light scattering measurements.

Supporting Information Available: CD, UV−vis, and linear dichroism spectra related to Figure 5. This material is available free of charge via the Internet at http://pubs.acs.org.

References and Notes

(1) (a) Keller, A.; Cheng, S. Z. D. *Polymer* **1998**, *39*, 4461. (b) Sirota, E. B.; Herhold, A. B. *Science* **1999**, *283*, 529–532.
(2) (a) Schaper, A.; Georgalis, Y.; Umbach, P.; Raptis, J.; Saenger, W. *J. Chem. Phys.* **1997**, *106*, 8587–8494. (b) Allegra, G.; Meille, S. V. *Adv. Polym. Sci.* **2005**, *191*, 87–135.
(3) (a) Häfele, A.; Heck, B.; Kawai, T.; Kohn, P.; Strobl, G. *Eur. Phys. J. E* **2005**, *16*, 207–216. (b) Yang, L.; Somani, R. H.; Sics, I.; Hsiao, B. S.; Kolb, R.; Lohse, D. *J. Phys.: Condens. Matter* **2006**, *18*, S2421–S2436. (c) Somani, R. H.; Yang, L.; Hsiao, B. S. *Phys. A* **2002**, *304*, 145–157. (d) Horn, D.; Rieger, J. *Angew. Chem., Int. Ed.* **2001**, *40*, 4330–4361.
(4) Balzano, L.; Kukalyekar, N.; Rastogi, S.; Peters, G. W. M.; Chadwick, J. C. *Phys. Rev. Lett.* **2008**, *100*, 048302.
(5) (a) McCulloch, I.; Heeney, M.; Bailey, C.; Genevicius, K.; Macdonald, I.; Shkunov, M.; Sparrowe, D.; Tierney, S.; Wagner, R.; Zhang, W. M.; Chabinyc, M. L.; Kline, R. J.; Mcgehee, M. D.; Toney, M. F. *Nat. Mater.* **2006**, *5*, 328–333. (b) Schwartz, B. J. *Annu. Rev. Phys. Chem.* **2003**, *54*, 141–172. (c) Hoeben, F. J. M.; Jonkheijm, P.; Meijer, E. W.; Schenning, A. P. H. J. *Chem. Rev.* **2005**, *105*, 1491–1546.
(6) Wu, L.; Sato, T.; Tang, H.-Z.; Fujiki, M. *Macromolecules* **2004**, *37*, 6183–6188.
(7) (a) Abbel, R.; Schenning, A. P. H. J.; Meijer, E. W. *Macromolecules* **2008**, *41*, 7497–7504. (b) Oda, M.; Nothofer, H.-G.; Lieser, G.; Scherf, U.; Meskers, S. C. J.; Neher, D. *Adv. Mater.* **2000**, *12*, 362–365.
(8) (a) Grimsdale, A. C.; Müllen, K. *Adv. Polym. Sci.* **2008**, *212*, 1–48. (b) Knaapila, M.; Winokur, M. J. *Adv. Polym. Sci.* **2008**, *212*, 227–272. (c) Scherf, U.; List, E. *Adv. Mater.* **2002**, *14*, 477–487. Neher, D. *Macromol. Rapid Commun.* **2001**, *22*, 1365–1385. (d) Grell, M.; Bradley, D. D. C.; Inbasekaran, M.; Woo, E. P. *Adv. Mater.* **1997**, *9*, 798–802. (e) Monkman, A. P.; Rothe, C.; King, S.; Dias, F. *Adv. Polym. Sci.* **2008**, *212*, 187–225.
(9) (a) Grell, M.; Bradley, D. D. C.; Ungar, G.; Hill, J.; Whitehead, K. S. *Macromolecules* **1999**, *32*, 5810–5817. (b) Chen, S. H.; Su, A. C.; Chen, S. A. *J. Phys. Chem. B* **2005**, *109*, 10067–10072. (c) Dias, F. B.; Morgado, J.; Macanita, A. L.; Da Costa, F. P.; Burrows, H. D.; Monkman, A. P. *Macromolecules* **2006**, *39*, 5854–5864.
(10) Chunwaschirasiri, W.; Tanto, B.; Huber, D. L.; Winokur, M. J. *Phys. Rev. Lett.* **2005**, *94*, 107402.
(11) (a) Peet, J.; Brocker, E.; Xu, Y.; Bazan, G. C. *Adv. Mater.* **2008**, *20*, 1882–1885. (b) O'Carroll, D.; Iacopino, D.; O'Riordan, A.; Lovera, P.; O'Connor, É.; O'Brien, G. A.; Redmond, G. *Adv. Mater.* **2008**, *20*, 42–48.
(12) Chen, S. H.; Su, A. C.; Su, C. H.; Chen, S. A. *J. Phys. Chem. B* **2006**, *110*, 4007–4013.
(13) Wu, C.; Wu, B. Chapter 1: Dynamic Light Scattering. In *Experimental Methods in Polymer Science*; Tanaka, T., Ed.; Academic Press: San Diego, **1998**.
(14) See the Supporting Information.
(15) Bright, D. W.; Dias, F. B.; Galbrecht, F.; Scherf, U.; Monkman, A. P. *Adv. Funct. Mater.* **2009**, *19*, 67–73.
(16) Paolantoni, M.; Sassi, P.; Morresi, A.; Cataliotti, R. S. *Mol. Phys.* **2001**, *99*, 1493–1502.
(17) Engel, J.; Bächinger, H. P. *Top. Curr. Chem.* **2005**, *247*, 7–34.
(18) Tang, H. Z.; Fujiki, M.; Sato, T. *Macromolecules* **2002**, *35*, 6439–6445.
(19) (a) Percec, V.; Aqad, E.; Peterca, M.; Rudick, J. G.; Lemon, L.; Ronda, J. C.; Heiney, B. B.; Meijer, P. A. *J. Am. Chem. Soc.* **2006**, *128*, 16365–16372. (b) Ciardelli, F.; Lanzillo, S.; Pieroni, O. *Macromolecules* **1974**, *7*, 174–179.
(20) (a) Knaapila, M.; Torkelli, M.; Monkman, A. P. *Macromolecules* **2007**, *40*, 3610. (b) Knaapila, M.; Stepanyan, R.; Lyons, B. P.; Torkkeli, M.; Monkman, A. P. *Adv. Funct. Mater.* **2006**, *16*, 599–609.
(21) (a) Marcon, V.; van der Vegt, N.; Wegner, G.; Raos, G. *J. Phys. Chem. B* **2006**, *110*, 5253–5261. (b) Oda, M.; Nothofer, H.-G.; Scherf, U.; Sunjic, V.; Richter, D.; Regenstein, W.; Neher, D. *Macromolecules* **2002**, *35*, 6792–6798.
(22) Berova, N.; Nakanishi, K.; Woody R. W. *Circular Dichroism: Principles and Applications*; Wiley-VCH: Weinheim, **2000**.
(23) Geng, Y.; Trajkovska, A.; Katsis, D.; Ou, J. J.; Culligan, S. W.; Chen, S. H. *J. Am. Chem. Soc.* **2002**, *124*, 8337–8347.